

Stratified horizontal flow in vertically vibrated granular layers

M. Levanon and D. C. Rapaport*

Physics Department, Bar-Ilan University, Ramat-Gan 52900, Israel

(Received 11 September 2000; published 18 June 2001)

A layer of granular material on a vertically vibrating sawtooth-shaped base exhibits horizontal flow whose speed and direction depend on the parameters specifying the system in a complex manner. Discrete-particle simulations reveal that the induced flow rate varies with height within the granular layer and oppositely directed flows can occur at different levels. The behavior of the overall flow is readily understood once this feature is taken into account.

DOI: 10.1103/PhysRevE.64.011304

PACS number(s): 45.70.Mg, 02.70.Ns

Understanding the static and dynamic properties of granular materials is a challenging task [1] and many aspects of their behavior are unexpected. An example of this kind of behavior is provided by a granular layer that is vibrated vertically by a base whose surface profile has a sawtooth form; in this particular case the material is confined to the annular region between two upright cylinders and is thus practically two dimensional. What is observed [2,3], both in experiment and computer simulation, is horizontal flow. While this effect is perhaps not entirely unexpected because the shape of the base breaks the horizontal symmetry, the complex manner in which the flow direction and magnitude depend on the many parameters that specify the system is surprising. The purpose of this paper is to describe a series of simulations that resolve this apparent complexity in terms of the flows in horizontal strata within the vibrated layer; when this hitherto unreported aspect of the behavior is taken into account the apparently complex nature of the overall flow ceases to be a mystery.

The problem of a vibrating granular layer on a flat base is an example of a granular system where it has proved possible both to validate the simulational approach based on suitable discrete-particle models and to use simulation to probe details of the dynamics that are not readily accessible to experiment; the standing wave patterns that occur in this system have been studied in two [4–6] and three [7,8] dimensions. When the sinusoidally oscillating base is given a sawtooth surface profile [2,3], horizontal flow appears; experiment and simulation both display the complex dependence of the flow direction and magnitude on the parameters defining the system. (While it is also possible to produce horizontal flow by combining horizontal and vertical base vibration [9], this is distinct from the sawtooth problem where the vibration is entirely vertical.) The sawtooth base can be regarded as a kind of ratchet; evidence of the complexity of systems involving potentials that produce ratchetlike effects appears in much simpler one-dimensional systems [10,11].

In the present series of two-dimensional simulations the interaction specifying the grain shape is assumed [12] to have a Lennard-Jones (LJ) form, with a cutoff at the range where the repulsive force falls to zero. For grains located at \mathbf{r}_i and \mathbf{r}_j this is $\mathbf{f}_{ij}^r = (48\epsilon/r_{ij})[(\sigma_{ij}/r_{ij})^{12} - 0.5(\sigma_{ij}/r_{ij})^6]\hat{\mathbf{r}}_{ij}$

for $r_{ij} < 2^{1/6}\sigma_{ij}$ and zero otherwise; here $\mathbf{r}_{ij} = \mathbf{r}_i - \mathbf{r}_j$ and $\sigma_{ij} = (\sigma_i + \sigma_j)/2$. σ_i is the approximate diameter of grain i , since the grains possess a certain degree of softness, this is not precisely defined. The LJ interaction is strongly repulsive at small r_{ij} , more so than the linear overlap and Hertzian type repulsions also used in granular simulation [13]. For convenience, we use reduced units in which length is expressed in terms of the diameter of the largest grains, energy in terms of ϵ , and a grain with unit diameter (in reduced units) has unit mass. Grain sizes are randomly distributed between 0.9 and 1.

Normal and transverse viscous damping forces [14,15] produce the inelastic collisions and retard sliding during the collision. The normal force is $\mathbf{f}_{ij}^n = -\gamma_n(\dot{\mathbf{r}}_{ij} \cdot \hat{\mathbf{r}}_{ij})\hat{\mathbf{r}}_{ij}$. The transverse force is $\mathbf{f}_{ij}^t = -\text{sgn}(v_{ij}^s)\min(\mu|\mathbf{f}_{ij}^n + \mathbf{f}_{ij}^t|, \gamma_s|v_{ij}^s|)\hat{\mathbf{s}}_{ij}$, where $v_{ij}^s = \dot{\mathbf{r}}_{ij} \cdot \hat{\mathbf{s}}_{ij} + r_{ij}(\sigma_i\omega_i + \sigma_j\omega_j)/(\sigma_i + \sigma_j)$ is the relative tangential velocity of the disks, $\hat{\mathbf{s}}_{ij} = \hat{\mathbf{z}} \times \hat{\mathbf{r}}_{ij}$ ($\hat{\mathbf{z}}$ is the unit normal to the simulation plane), and ω_i is an angular velocity. The value of the static friction coefficient used here is $\mu = 0.5$ and the normal and transverse damping coefficients are $\gamma_n = \gamma_s = 5$.

While most granular simulations are based on particles with a certain amount of softness, allowing the use of differentiable potentials, there is an alternative approach involving step potentials; provided the former are not too soft and the flow involves some degree of fluidization the results of the two approaches are similar [16,17]. The previous simulations of the sawtooth problem [3] used step potentials and the results were limited to thin layers; the softer potentials of the present work do not restrict the layer thickness.

The sawtooth base is constructed from a set of grainlike disks positioned to produce the required profile; these disks oscillate vertically in unison to produce the effect of a sinusoidally vibrated base. The disks themselves interact with the grains using the same force laws as above; their diameter is 0.33 and the distance between disk centers is half of this value, producing sawtooth edges that are reasonably straight. The system is horizontally periodic and extends sufficiently far vertically to prevent grains reaching the upper boundary.

Gravity also acts on the grains; here $g = 5$. The total force and torque on each grain are readily computed and the equations for translational and rotational motion are numerically integrated using the leapfrog method with a time step of

*Electronic address: rapaport@mail.biu.ac.il

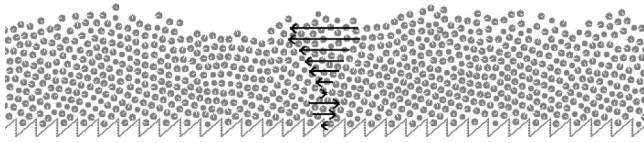


FIG. 1. Screen snapshot showing a portion of a typical system.

0.005. These and other methodological issues are described elsewhere [18]. Each run extends over 1000 base cycles and the results are grouped into 10 nonoverlapping blocks to provide error estimates. (The reduced units employed here can be related to physical units. If, for example, the particle diameter is actually 10^{-3} m, then the reduced time unit consistent with the choice of $g=5$ corresponds to 0.022 s, and $f=0.5$ is equivalent to a frequency of ≈ 23 Hz. Other choices of length scale and g will lead to different time scales.)

The results described here are for a sawtooth height of 2 and a vibration amplitude of 1. The sawtooth shape is strongly asymmetric, with a gently sloping left edge and an almost vertical right edge; projected onto the base the edge lengths are in the ratio 99:1. The adjustable parameters considered here are the base vibration frequency f and the number of sawteeth s (s is specified rather than the tooth width since it must be an integer). The initial state consists of grains positioned on a rectangular grid with unit spacing; the horizontal grid size is fixed at 90 (this is also the system width), and the adjustable vertical grid size is taken to be the nominal thickness h of the granular layer.

Figure 1 shows a screen image (with limited visual resolution) of a portion of a typical system for the case $s=40$. Since the base is near its lowest point the surface wave form is absent. The arrows indicate the stratified flow discussed below.

Figure 2 shows a contour plot of the average horizontal flow velocity as a function of f (frequency) and s (number of teeth) for layer thickness $h=4$. The flow is negative at low s , and for certain f also at high s (corresponding to narrow gaps between teeth with space for just a single grain); horizontal cuts through the plot for certain s values show velocity reversals as a function of f , likewise, vertical cuts show reversals as a function of s . Figure 3 is similar but for $h=10$; the flow is stronger at low f and there is a larger negative region at high s . Examination of the entire range of h values considered (between 1 and 16) reveals smoothly shifting domain boundaries separating positive and negative flows; merely examining a few cuts through these multidimensional plots will miss this gradual variation. These results include the complex parameter dependence observed previously in both experiment and simulation [2,3], but with reversed signs because of the opposite sawtooth asymmetry.

The results shown in Fig. 4 deal with another two-dimensional cross section through the multidimensional parameter space and reveal the flow dependence on s and h for $f=0.5$. Flow reversals are seen to occur both as functions of s and h (including the $h=1$ monolayer). Other values of f over the range examined (0.3 to 0.7) again show a gradual shifting of the boundaries between regions of oppositely directed flow.

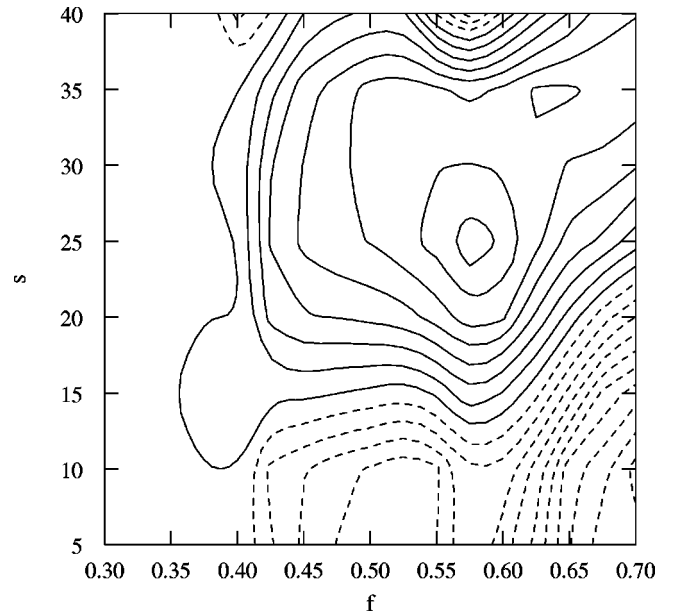


FIG. 2. Contour plot showing overall horizontal flow velocity as a function of f and s for $h=4$ (in reduced units); solid and dashed curves denote positive and negative values, respectively, and the contour interval is 0.013 (the same value is used subsequently).

Space precludes discussion of the corresponding results for other parameter choices (such as sawtooth height and asymmetry) that are similar in essence but differ in detail. A particularly drastic change is to set the tangential damping to zero, thereby removing the rotational component of the dynamics. Once again the quantitative details change, but the overall behavior is not strongly affected; the main effect of rotation and the associated damping is to increase energy dissipation. Similar results are also obtained when the interaction used here is replaced by a linear overlap repulsion.

Further progress in understanding the behavior requires

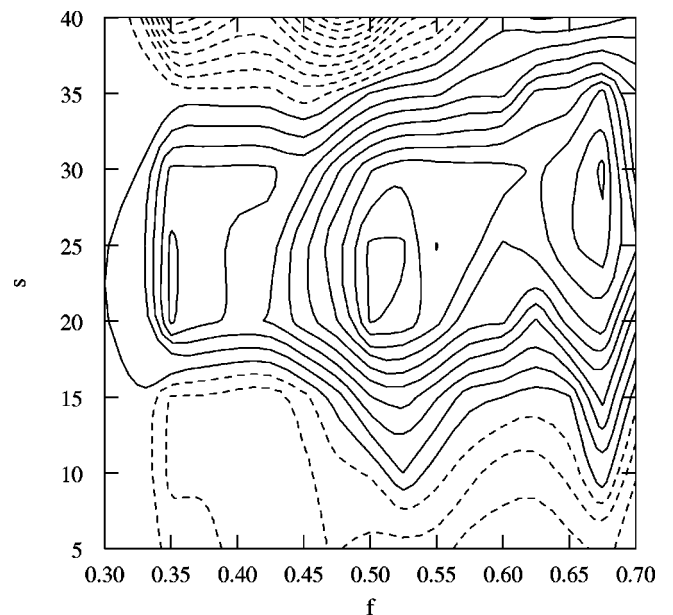


FIG. 3. Flow velocity (see Fig. 2) for $h=10$.

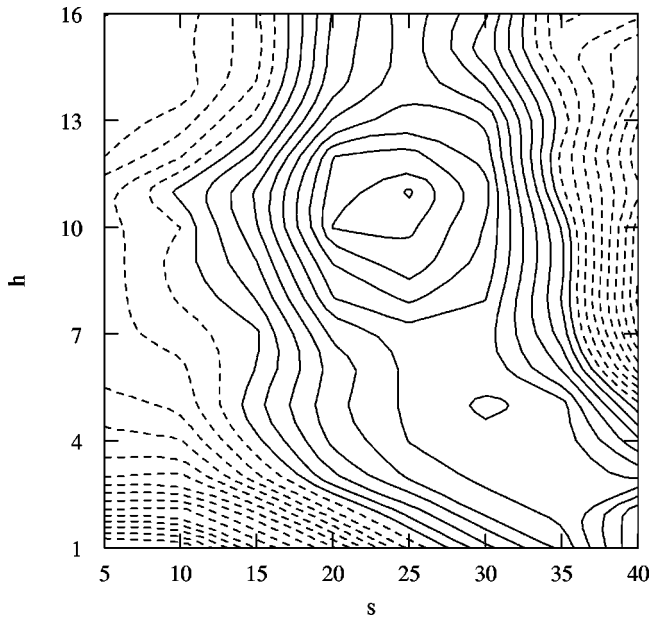


FIG. 4. Flow velocity as a function of s and h for $f=0.5$.

looking beyond the overall flow and taking advantage of the simulations to examine the dynamics in greater detail. An analogy can be made with thermal convection where the mean flow is zero, but this does not preclude the presence of highly structured convection rolls. Here, too, there are localized flow structures that can only be detected by probing the spatial variation of the flow; Fig. 1 already hinted at the kind of behavior that can be observed if flows in distinct horizontal strata are measured. The experiments carried out on this system [2,3] examined just the overall flow by measuring tracer particle motion, and the accompanying simulations were confined to thin layers only, so there was little opportunity for observing any spatial variation.

Studying stratified flow requires assigning grains to horizontal levels while allowing for the fact that grains can migrate vertically. Since this procedure is not uniquely defined, the approach adopted here is to reassign the grains once every vibration cycle when the base reaches its lowest point. This has certain shortcomings, particularly for higher f , because grains in the peaks of the surface waves are assigned to higher levels; however, apart from some smearing of the measurements between levels, no spurious effects are expected from this approach.

Figure 5 shows the height (z) dependence of the stratified flow velocity for $h=8$, for several sets of f and s values; the thickness of each level is 1.2, which is slightly larger than the grain size. Figure 6 shows the corresponding results for $h=12$. A typical velocity profile starts with a slightly negative or near-zero flow at the bottom level; the flow initially increases with z , reaches a positive maximum, and then starts to drop, in most cases eventually becoming negative again. (In physical units the horizontal flow speeds are of order 10^{-2} m/s.) The curves for $s=10$ (wide teeth) and $s=40$ (narrow teeth) are the most negative at the upper levels, while intermediate curves show strong positive maxima near $z=4$.

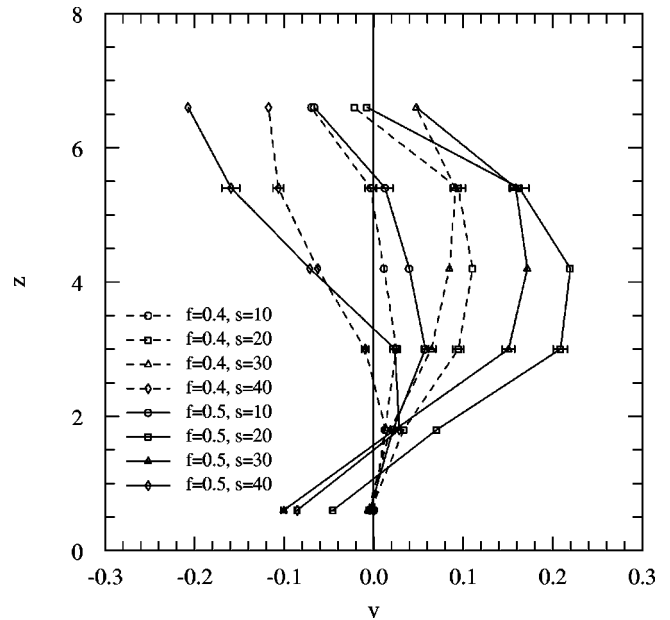


FIG. 5. Stratified flow velocity (v) as a function of height (z) above the base for $h=8$; typical error bars are shown.

The preferred flow directions at different levels reflect the key features of the system. The behavior of the grains near the base is reminiscent of a thin layer that can flow in either direction, depending on the prevailing conditions, although it is generally dominated by a ratcheting effect in which grains tend to move in the positive direction by climbing up the shallow tooth faces. On the other hand, the asymmetry of the sawteeth, which in themselves would be more likely to reflect falling grains in the negative direction, indirectly influences the behavior in the upper levels; this effect is transferred through the intervening material that could well be moving in the positive direction. When positive flow occurs

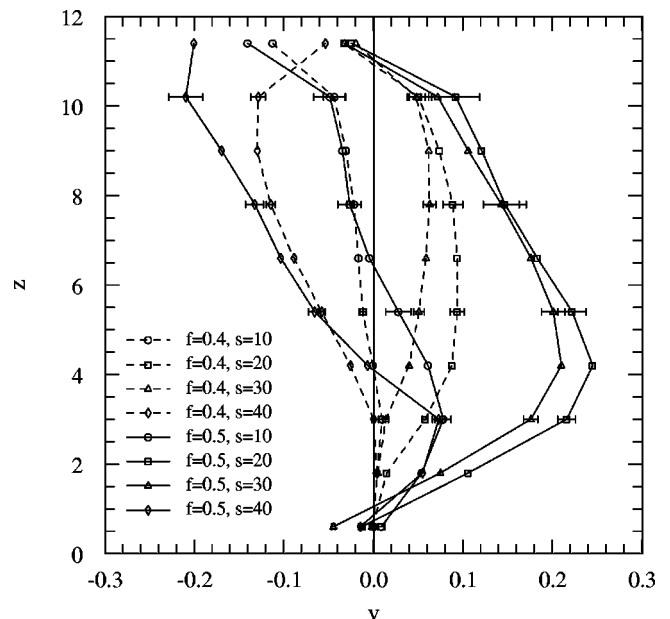


FIG. 6. Stratified flow velocity (see Fig. 5) for $h=12$.

at the lower levels the competition between these opposing effects produces the counterflowing velocity profile. This idealized scheme is of course complicated by other aspects, including grain rotation and the fact that the grains at the bottom can become trapped between the teeth thereby reducing the effective sawtooth height.

The explanation for the puzzling reversals in the overall flow direction is embodied in curves such as those shown in Figs. 5 and 6. The average flow is simply the density-weighted mean of the stratified flow velocity; its sign depends on the detailed form of the velocity profile and is a consequence of the relative strengths of the positive and negative flows occurring at different levels. Since only a slight change in the profile may be enough to produce a reversal of the overall flow direction, the sensitive parameter dependence is hardly surprising.

In general, the more familiar role of simulation, particularly as it applies to granular media, is in attempting to reproduce experimentally observed behavior. In this paper the process has been inverted, and through simulation it has proved possible to identify a previously unknown transport mechanism in a model of a vibrated granular system. On the assumption that the model correctly describes the relevant features of real granular materials, this amounts to a prediction that calls for experimental verification. Should this kind of behavior be found experimentally, stratified flow would be an interesting addition to the extensive repertoire of exotic properties exhibited by granular matter.

This research was supported in part by the Israel Science Foundation. We are grateful to T. Vicsek for introducing us to the problem.

-
- [1] H. M. Jaeger, S. R. Nagel, and R. P. Behringer, *Rev. Mod. Phys.* **68**, 1259 (1996).
 - [2] I. Derényi, P. Tegzes, and T. Vicsek, *Chaos* **8**, 657 (1998).
 - [3] Z. Farkas, P. Tegzes, A. Vukics, and T. Vicsek, *Phys. Rev. E* **60**, 7022 (1999).
 - [4] E. Clément, L. Vanel, J. Rajchenbach, and J. Duran, *Phys. Rev. E* **53**, 2972 (1996).
 - [5] S. Luding, E. Clément, J. Rajchenbach, and J. Duran, *Europhys. Lett.* **36**, 247 (1996).
 - [6] D. C. Rapaport, *Physica A* **249**, 232 (1998).
 - [7] C. Bizon, M. D. Shattuck, J. B. Swift, W. D. McCormick, and H. L. Swinney, *Phys. Rev. Lett.* **80**, 57 (1998).
 - [8] C. Bizon, M. D. Shattuck, J. R. de Bruyn, J. B. Swift, W. D. McCormick, and H. L. Swinney, *J. Stat. Phys.* **93**, 449 (1998).
 - [9] J. A. C. Gallas, H. J. Herrmann, and S. Sokolowski, *J. Phys. II* **2**, 1389 (1992).
 - [10] C. R. Doering, W. Horsthemke, and J. Riordan, *Phys. Rev. Lett.* **72**, 2984 (1994).
 - [11] I. Derényi and T. Vicsek, *Phys. Rev. Lett.* **75**, 374 (1995).
 - [12] D. Hirshfeld and D. C. Rapaport, *Phys. Rev. E* **56**, 2012 (1997).
 - [13] J. Schäfer, S. Dippel, and D. E. Wolf, *J. Phys. I* **6**, 5 (1996).
 - [14] P. A. Cundall and O. D. L. Strack, *Geotechnique* **29**, 47 (1979).
 - [15] O. R. Walton, in *Mechanics of Granular Materials*, edited by J. T. Jenkins and M. Satake (Elsevier, Amsterdam, 1983), p. 327.
 - [16] S. Luding, H. J. Herrmann, and A. Blumen, *Phys. Rev. E* **50**, 3100 (1994).
 - [17] S. Luding, E. Clément, A. Blumen, J. Rajchenbach, and J. Duran, *Phys. Rev. E* **50**, R1762 (1994).
 - [18] D. C. Rapaport, *The Art of Molecular Dynamics Simulation* (Cambridge University Press, Cambridge, 1995).